

**Figure 1** Computer simulations of the model<sup>1</sup> with  $N=100$  individuals,  $D$  phenotypic defectors and different costs of cooperation  $c$ . **a–d**, Average strategy  $\langle k \rangle$  of the population over a simulation of 100,000 generations for different  $c$  and  $D$ . **e**, Frequency distribution of strategies sampled over  $10^7$  generations with low, intermediate and high costs of cooperation, and with various numbers of phenotypic defectors,  $D$ . Model parameters are as in ref. 1, with  $b=1$ , mutation rate  $\mu=0.001$ , and  $m=300$  random interactions per generation. As in ref. 1, after every generation the number of offspring of each player is determined by the fitness accumulated over a lifetime of interactions, and the population strategies evolve by selection and mutation over many generations.

$k = +6$  (pure defection), with  $k=0$  indicating a ‘discriminating’ strategy. The cost to the donor’s fitness for each cooperation is  $c$  and the recipient’s benefit is  $b$ .

We modified this scheme and allowed a population of  $N=100$  individuals to carry  $D$  phenotypic defectors. We assigned the non-heritable phenotypic strategy  $k = +7$  to  $D$  randomly chosen individuals every generation, but we left unchanged the heritable genotypic strategies of these defectors.

We first consider the effects of phenotypic defectors in a model in which the costs of cooperation are intermediate compared with the benefit of the beneficiary ( $c=0.35, b=1$ ). In the absence of phenotypic defectors ( $D=0$ ), the simulation model<sup>1</sup>, which incorporates mutation and drift, generally results in a population consisting almost entirely of defectors (Fig. 1a). However, upon the introduction of  $D=10$  phenotypic defectors, the population structure becomes dominated by discriminating altruists whose average strategy is mostly  $\langle k \rangle = 0$  (Fig. 1b). Over  $10^7$  generations, the introduction of phenotypic defectors increases the overall frequency of discriminators ( $\langle k \rangle = 0$ ) from 12% ( $D=0$ ) to 74% ( $D=10$ ) and even 95% ( $D=20$ ) (Fig. 1e, middle). These results demonstrate that phenotypic defectors, who are unable to

provide help, may nevertheless be central to the evolution of cooperation.

We turn now to the model in which the cost of cooperation is relatively low<sup>1</sup> ( $c=0.1$ ). With no phenotypic defectors ( $D=0$ ), the simulation model yields long-term cycling in the average strategy index, generally with cooperative populations ( $\langle k \rangle \leq 0$ ), but with defectors invading occasionally (Fig. 1c). Although the population initially consisted mostly of cooperators, the introduction of 20 phenotypic defectors led to discriminating cooperators being favoured (at  $\langle k \rangle = -1$ ), effectively suppressing this cycling dynamic (Fig. 1d).

The paradoxical effect whereby phenotypic defectors stabilize discriminate altruism can be explained analytically (see <http://lynx.tau.ac.il/coop.html>). Whenever there are defectors in the population, there is a persistent advantage for discriminators over non-discriminating altruists because discriminators avoid paying the costs of helping defectors. This advantage disappears as soon as all defectors are eliminated from the population, as often occurs in the Nowak and Sigmund model<sup>1</sup>. In our model, however, a constant supply of phenotypic defectors ensures that the advantage persists, leading to a large population of discriminators that deny help to real genotypic defectors and hence block their invasion.

Our study also shows that the qualitative effect of phenotypic defectors is highly dependent on the cost of cooperation,  $c$  (Fig. 1e). A high cost ( $c=0.7$ ) leads to a population of defectors ( $\langle k \rangle > 0$ ) no matter how many phenotypic defectors  $D$  are added. However, for intermediate costs ( $c=0.35$ ), the addition of only a few phenotypic defectors strongly increases discriminate altruism (Fig. 1b, e). For low costs ( $c=0.1$ ), where the population is initially cooperative with long-term cycling (when  $D=0$ ), the addition of phenotypic defectors tends to suppress the cycling dynamic.

In the Nowak and Sigmund model<sup>1</sup>, the relative frequencies of discriminators and non-discriminators fluctuate during the long-term population cycling, whereas our model predicts that, in cooperative societies, non-discriminators will be replaced by discriminators when the cost of cooperation increases. This implies the evolution of a society in which cheap donations are given unconditionally to everyone, whereas more costly gifts are given discriminatingly, and only to those individuals who can afford to donate such gifts to others (those who are in good phenotypic condition). Evidence for costly help being provided unconditionally to poor phenotypes may not be explained by indirect reciprocity, but rather by alternative theories<sup>3–5</sup>.

**Arnon Lotem, Michael A. Fishman, Lewi Stone**

Department of Zoology, Faculty of Life Sciences, Tel-Aviv University, Tel-Aviv 69978, Israel  
e-mail: lotem@post.tau.ac.il

1. Nowak, M. A. & Sigmund, K. *Nature* **393**, 573–577 (1998).
2. Nowak, M. A. & Sigmund, K. *J. Theor. Biol.* **194**, 561–574 (1998).
3. Hamilton, W. D. *J. Theor. Biol.* **7**, 1–52 (1964).
4. Zahavi, A. in *Evolutionary Ecology* (ed. Stonehouse, B. & Perrins, C. M.) 253–259 (Macmillan, London, 1977).
5. Roberts, G. *Proc. R. Soc. Lond. B* **265**, 427–431 (1998).

## Higher fullerenes in the Allende meteorite

Fullerenes ( $C_{60}$  and  $C_{70}$ ) were discovered during investigations of the mechanism by which carbon molecules form in interstellar and circumstellar shells<sup>1</sup>. Unlike diamond and graphite, the other pure forms of carbon, fullerenes are extractable in an organic solvent such as toluene, which led to the detection of the higher fullerenes ( $C_{100}$  to  $C_{250}$ ) in carbon-arc-evaporated soot material<sup>2</sup>. We have applied a similar solvent extraction procedure to an acid residue of the carbonaceous chondrite from the Allende meteorite to search for higher fullerenes. We found  $C_{60}$  and  $C_{70}$ , as well as a unique distribution of remarkably stable clusters of  $C_{100}$  to  $C_{400}$ . These large extraterrestrial carbon clusters are either the first indication of higher fullerenes or are an

entirely new range of aromatic carbon-rich molecules.

Carbonaceous chondrites contain interstellar grains, including diamond, silica carbide (SiC), graphite and carbon-based molecules that were formed in stellar atmospheres, mixed into the Solar nebula, and incorporated into the meteorite matrix<sup>3</sup>. Fullerenes (C<sub>60</sub> and C<sub>70</sub>) measured in parts per billion, and possibly fulleranes (C<sub>60</sub>H<sub>x</sub>), have been detected in the Allende meteorite, indicating that they existed either in the early Solar nebula or as a component of pre-Solar dust<sup>4,5</sup>. Polycyclic aromatic hydrocarbons (PAHs) may also form in circumstellar environments<sup>6,7</sup>. Theories about the role of diamonds, graphite, SiC, PAHs, fullerenes and fulleranes have also been proposed to explain such phenomena as the diffuse interstellar bands.

Ascertaining how and where these carbon species form requires an assessment of the structure and stability of carbon clusters. For clusters of less than ten carbon atoms, linear structures are energetically favoured. At C<sub>10</sub> to C<sub>20</sub>, linear structures close into rings, but between C<sub>20</sub> and C<sub>30</sub> (the 'forbidden zone') it is unclear what structures are favoured<sup>7</sup>. For clusters with more than 30 carbon atoms, however, the lowest-energy structures, with up to several hundred carbon atoms, seem to favour aromatic and fullerene-related carbon cages<sup>7,8</sup>. Because the size range of interstellar PAHs

is limited owing to hydrogenation (at about 30 carbon atoms, individual PAHs may be fully hydrogenated, slowing growth as carbon atoms are added), and only trace levels of C<sub>60</sub> and C<sub>70</sub> have been detected in a single carbonaceous chondrite<sup>4,5</sup>, the search has now turned to the larger clusters (carbon 'onions' and nanotubes) as a possible carrier of noble gases and as a higher-molecular-mass carbon component in meteorites. We have searched for fullerenes and larger clusters in both the toluene extract and the acid-insoluble residue (extracted with 1,2,4-trichlorobenzene; TCB) generated from the Allende meteorite. Laser desorption (linear) time-of-flight mass spectrometry (LDMS) was used to detect fullerenes (C<sub>60</sub> and C<sub>70</sub>) and any higher-molecular-mass carbon clusters.

LDMS analyses of the toluene extract revealed peaks at C<sub>60</sub><sup>+</sup> and C<sub>70</sub><sup>+</sup>, confirming our earlier results<sup>5</sup> on a separate acid-treated split of the Allende meteorite. In addition, C<sub>74</sub><sup>+</sup>, C<sub>76</sub><sup>+</sup>, C<sub>78</sub><sup>+</sup> and C<sub>84</sub><sup>+</sup> were detected at a factor of 2–3 below C<sub>60</sub><sup>+</sup> and C<sub>70</sub><sup>+</sup>, as well as several mass peaks in the *m/z* range 100 to 400 atomic mass units, indicating the presence of PAHs and their methyl derivatives<sup>4,5</sup>. LDMS analysis (Fig. 1a) revealed peaks for C<sub>60</sub><sup>+</sup>, C<sub>70</sub><sup>+</sup> and some higher fullerenes (C<sub>76</sub><sup>+</sup> to C<sub>96</sub><sup>+</sup>) and a more prominent high-mass envelope extending from C<sub>100</sub><sup>+</sup> to C<sub>250</sub><sup>+</sup>. Closer examination of the larger carbon clusters (Fig. 1b) revealed

a large repeating peak pattern separated by about 24 atomic mass units. These clusters are separated by C<sub>2</sub><sup>+</sup> units, indicating that the high-mass envelope detected in the toluene-insoluble TCB residue is due to pure carbon clusters<sup>2</sup>.

This idea is supported by considering the composition of the TCB-extracted Allende residue. In general, the insoluble carbon component of carbonaceous chondrites (CI, CM, CO and CV) is a 'macromolecular material' containing hydrogen, nitrogen, oxygen, sulphur and perhaps halogens, as well as carbon<sup>9</sup>. However, the Allende meteorite appears to be the limiting case in that the principal insoluble component is elemental carbon, which differs from graphite in having a poorly ordered structure (sp<sup>2</sup>-hybridized carbon)<sup>10</sup>. It is this insoluble material that retains the high-mass carbon clusters seen in Fig. 1a,b when extracted with TCB. The Allende residue also has several well-ordered graphitic particles that are similar in size and appearance to carbon onions and nanotubes<sup>9</sup>.

It seems that fullerenes and higher-carbon clusters are indeed formed in the outflows of carbon stars, as was suggested soon after their discovery<sup>1</sup>. Their presence in the Allende meteorite indicates that they can survive passage through space and subsequent processing in the interstellar medium, and the accretion process into grains and larger bolides (such as asteroids or meteorites), as well as arriving on planets such as Earth. Fullerenes and higher-carbon clusters may have been important on the early Earth, and perhaps other planets, by providing not only a source of carbon, an essential element for life, but also the volatiles that contributed to the planetary atmospheres needed for the origin of life<sup>11</sup>.

**Luann Becker\***, **Theodore E. Bunch†**,  
**Louis J. Allamandola†**

\*Hawaii Institute of Geophysics and Planetary Sciences, University of Hawaii,

2525 Correa Road, Honolulu, Hawaii 96822 USA

e-mail: lbecker@soest.hawaii.edu

†Space Science Division,

NASA Ames Research Center, Moffett Field,

California 94305, USA

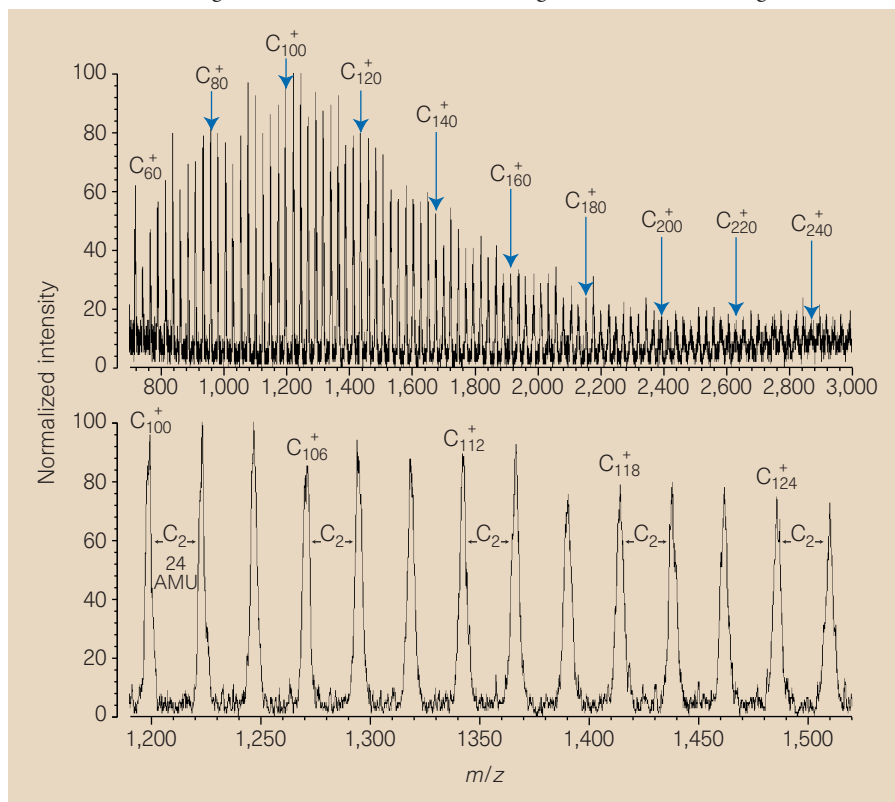


**Figure 1** LDMS mass spectra for the TCB extract of the Allende meteorite. **a**, Spectra showing a small peak for C<sub>60</sub><sup>+</sup> and a range of remarkably stable larger carbon clusters between C<sub>100</sub><sup>+</sup> and C<sub>250</sub><sup>+</sup> (clusters were observed up to C<sub>400</sub><sup>+</sup>). **b**, Closer examination of the larger clusters. For more details, see Supplementary Information.

1. Kroto, H. W., Heath, J. R., O'Brien, S. C., Curl, R. F. & Smalley, R. E. *Nature* **318**, 162–163 (1985).
2. Diederich, F. & Whetten, R. *Acc. Chem. Res.* **25**, 119–126 (1992).
3. Zinner, E., Amari, S., Wopenka, B. & Lewis, R. S. *Meteoritics* **30**, 209–226 (1995).
4. Becker, L., Bada, J. L., Winans, R. E. & Bunch, T. E. *Nature* **372**, 507 (1994).
5. Becker, L. & Bunch, T. E. *Meteorit. Planet. Sci.* **32**, 479–487 (1997).
6. Leger, A. & Puget, J. L. *Astrophys. Lett.* **137**, L5–L8 (1984).
7. Curl, R. F. *Phil. Trans. R. Soc. Lond. A* **343**, 19–32 (1993).
8. O'Brien, S. C., Heath, J. R., Curl, R. F. & Smalley, R. E. *J. Chem. Phys.* **88**, 220–230 (1987).
9. Cronin, J. R., Pizzarello, S. & Cruikshank, D. P. in *Meteorites and the Early Solar System* (eds Kerridge, J. F. & Matthews, M. S.) 819–857 (Univ. Arizona Press, Tucson, 1986).
10. Smith, P. & Buseck, P. R. *Science* **212**, 322–324 (1981).
11. Becker, L., Poreda, R. J. & Bada, J. L. *Science* **272**, 249–252 (1996).

Supplementary information is available on Nature's World-Wide Web site (<http://www.nature.com>) or as paper copy from the London editorial office of Nature.